Transportation Research Part C 150 (2023) 104105

Contents lists available at ScienceDirect

Transportation Research Part C

journal homepage: www.elsevier.com/locate/trc

Throughput properties and optimal locations for limited deployment of Max-pressure controls

Simanta Barman *, Michael W. Levin [1]

Department of Civil, Environmental, and Geo- Engineering, University of Minnesota, MN 55455, USA

ARTICLE INFO

Keywords:
Max-pressure
Backpressure
Intersection
Deployment
Budget

ABSTRACT

Max-pressure (MP) control is one of the few traffic signal controllers proven to maximize network throughput or maximally stabilize the network. According to the theoretical results published so far, it can stabilize a network if all intersections are equipped with MP control for all stabilizable demands. However, budget constraints may not allow the installation of MP control on all intersections. Previous work did not consider a limited number of MP controlled intersections while proving the stability properties. Therefore, it is not clear whether a network can still be stabilized with a limited deployment of MP control. Using Lyapunov drift techniques this paper proves that even with a limited deployment, MP control can stabilize a network within feasible demand. Then we present an optimization formulation to find the optimal intersections to install MP control given a limited budget. We also present a greedy efficient algorithm to solve that optimization problem and prove that the algorithm solves the problem to optimality. Numerical results from simulations conducted on the downtown Austin network using an in-house custom simulator called AVDTA are then presented. The change in theoretical maximum servable demands for different amounts of deployments obtained from the optimization problem seemed to match with simulation results most of the times. We found that limited deployment of MP control almost always performed better than random deployment of MP control in terms of servable stable demand. Average total queue length and link density were observed to decrease as the number of MP controls increased which indicates better network performance. Average travel times per vehicle also decreased with installations of MP controls which shows how the travelers would benefit from more MP controls.

1. Introduction

Traffic signal controllers play an important role in dealing with traffic congestion. Well-planned traffic signal control have shown to improve system performance significantly (Lioris et al., 2016; Levin and Boyles, 2017; Sun and Yin, 2018). Among the traffic signal controllers developed so far, very few controllers are proven to have theoretical maximum throughput guarantees. One such controller with this property is called Max-pressure (MP) control. The concept of MP control was introduced independently by Varaiya (2013) and Wongpiromsarn et al. (2012) in the context of traffic signal control. MP control is a maximally stable, adaptive, computationally efficient and decentralized (therefore also distributed) traffic signal control policy. A controller is stable for a network if over a large period of time the sum of the queues of vehicles is bounded for a feasible demand. Moreover, a controller is maximally stable for a network if the controller can stabilize all possible stabilizable demands. Here the feasible demands is the set

* Correspondence to: 275 Civil Engineering Building, 500 Pillsbury Drive S.E. Minneapolis, MN 55455, USA
E-mail addresses: barma017@umn.edu (S. Barman), mlevin@umn.edu (M.W. Levin).
[1] 140 Civil Engineering Building, 500 Pillsbury Drive S.E. Minneapolis, MN 55455.

https://doi.org/10.1016/j.trc.2023.104105
Received 2 August 2022; Received in revised form 12 March 2023; Accepted 12 March 2023
Available online 20 March 2023
0968-090X/© 2023 Elsevier Ltd. All rights reserved.

of all demands that can be served by some other controller including the theoretical controllers. So, the maximum stability property implies that the maximally stable control can serve all demands that can be theoretically served. A network of autonomous computers that are connected to each other and share complete or partial information about the network to perform necessary computation is a distributed system. A decentralized system is a specialization of distributed system where information about the whole network do not need to be shared. In a decentralized network, the autonomous computers can perform necessary computation just by using local information about the network. The MP control at each intersection can make throughput-optimal signal control decisions without communicating with other intersections which makes it a decentralized controller. The decentralized property ensures that no explicit communication between the intersections is needed which makes it scale really well for large networks.

Several papers have already presented numerical results (Levin and Boyles, 2017; Sun and Yin, 2018; Barman and Levin, 2022) indicating MP control performs better compared to other signal controllers. However, all of the papers so far used MP on all of the signalized intersections. Even though it would be ideal to install MP in all the intersections according to those results, it may not be feasible due to budget constraints. Budget and other installation constraints may only allow installing MP in some intersections. However, it is not clear how installing MP on some intersections would affect performance of the traffic network. Even though MP is proven to be maximally stable when all intersections have MP control, no stability guarantee exists in the literature when MP is installed on only some of the intersections. Along with nonexistent theoretical guarantees previous works do not consider a limited deployment of MP control in simulations either. This paper tries to deal with this exact problem. For maximum stability for limited deployment of MP control on n intersections we only consider the feasible demands obtained by improving the control on those n intersections. This means that we consider all the demand that the network can serve with any other controller installed on those n intersections while analyzing maximum stability. However, this feasible region is smaller than the feasible region where all the intersection's control are modifiable. To be precise, the term maximum stability for the limited deployment policy presented in this paper refers to maximum stability if only n intersections are modifiable. Can MP control still achieve maximum stability if it is used only on some of the intersections? How would the performance of the system be affected? These are some of the questions this paper tries to address. This paper also determines the optimal intersections to install MP control. The optimal order of installation is also determined which allows more MP control to be installed in the future as more budget becomes available. Being able to determine the best intersections given the budget and the order of installation of MP control provides practical engineering and planning advantages.

The literature does not contain any proof of stability or numerical results with a limited deployment of MP control. All previous studies used MP control on all of the signalized intersections. The contributions of this paper are the following: we prove that MP control achieves maximum stability even for a limited number of deployed MP controls when the average demand for a network is in the set of feasible demands. We also define the set of feasible demands mathematically and call it the stable region. We then present a mixed-integer-linear-programming (MILP) formulation to determine the optimal intersections for the installation of MP controls. A greedy algorithm is also proposed and shown to be able to efficiently solve the MILP to optimality. Numerical results validating the theoretical results are then presented for the downtown Austin network. We present the maximum stable demand under our deployment policy and a random deployment policy. We also present how the system performance is affected with more installations of MP controls as budget for deployment increases.

The remainder of this paper is organized as follows. Section 2 reviews the literature on MP control: how it has been used so far and what gaps in the literature still exists. Limited deployment is introduced in Section 3 mathematically and a proof of stability is provided. A MILP formulation to find the intersections where MP control should be deployed is provided in Section 4 along with a greedy solution algorithm. Numerical results from the theory and simulations are provided in Section 5. Finally, the conclusions of this study are presented.

2. Literature review

Tassiulas and Ephremides (1992) first developed a maximum stability control for a queueing network with interdependent servers. They also presented an algorithm called backpressure (BP) or max-pressure to control the dependency among the servers by activating a subset of the servers so that the network remains maximally stable. Varaiya (2013) and Wongpiromsarn et al. (2012) independently presented this algorithm in the context of traffic networks and proved that traffic networks can also be maximally stabilized using this control. The implications of their results include: 1. Most importantly, the network throughput would be maximized, 2. The traffic signals can be controlled in a decentralized manner, 3. The only historical data required is the turn proportions which can be estimated (Varaiya, 2013; Gregoire et al., 2014a). Independently, Gregoire et al. (2014b) proved MP control can maximally stabilize traffic networks and Gregoire et al. (2014a) showed the results of using the control on a 21×21 grid network. Their conclusions based on the simulation results was that the algorithm tends to stabilize a significant part of the capacity region and benefits of their algorithm originated more from the realistic assumptions on queue measurements. However, they did qualify that even though the control algorithm can stabilize traffic networks with demand in a certain demand region, according to the simulations it is still not the optimal control. Sha and Chow (2019) found that a centralized control based on store and forward queueing model with the objective to minimize global network queues by adjusting green splits outperforms MP control. However, with increasing awareness of the traffic condition the drivers reroute and this causes the difference between the performance from the centralized control and MP control to decrease. Nilsson and Como (2022) presented a class of dynamic and decentralized traffic signal control policies called generalized proportional allocation (GPA) with proof of maximum stability. For proving the throughput properties, they used the vertical or point queue link model. Nilsson and Como (2020) provided comparison between MP and GPA controllers. They found that while GPA outperformed MP control during low demand periods, during high demand periods MP control performed better in terms of total queue length of the network.

Varaiya (2013) and Gregoire et al. (2014a) assumed a store and forward queueing model with infinite queue capacity for the stability proofs. Other research has been conducted to make the assumptions more realistic. To handle noises in queue measurements Xiao et al. (2015b,a) developed extensions to the MP control with the proof of stability. Wu et al. (2018) gave a delay-based MP control with the proof of stability. To model traffic queues more accurately Xiao et al. (2014) used spatial queue link model with finite traffic queues for their stability proof and Gregoire et al. (2014b) used spatial queue link model for their analysis. Li and Jabari (2019) later used kinematic wave theory to get an even more accurate traffic model. Hao and Yang (2019) presented a new hierarchical multi-granularity traffic network with an extended MP control which outperformed fixed signal timing and acyclic MP control.

Several papers presented simulation results that showed that under different conditions, variations of MP control outperformed other traffic signal controls. Lioris et al. (2016) presented MP control as efficacious arterial traffic regulator, Gregoire et al. (2014a) presented MP control with unknown routing, Kouvelas et al. (2014), Sun and Yin (2018) and Ramadhan et al. (2020) presented different versions of MP controller's performance in simulation. Some papers presented capacity-aware (Gregoire et al., 2014b), utilization-aware (Chang et al., 2020), double pressure based (Yu et al., 2021), route choice included (Smith et al., 2019) versions of MP control that showed positive results. Some real experimental studies (Mercader et al., 2020; Dixit et al., 2020) also reported favorable results from different variations of MP control.

The phase change process using the acyclic MP control appears random to the drivers which causes many problems with real life implementation (Levin et al., 2020). To solve this problem several papers developed cyclic versions of MP control. Le et al. (2015) proved that MP control with fixed cycle time and cyclic phases can stabilize networks. Pumir et al. (2015), Anderson et al. (2018) and Levin et al. (2020) developed different versions of cyclic MP control. All of these cyclic MP control papers contained proof of stability. Xiao et al. (2020) presented a cyclic MP control that used multi-objective optimization and Xu et al. (2021b) presented a path based cyclic MP control. Barman and Levin (2022) and Robbennolt et al. (2022) compared several versions of acyclic and cyclic MP controllers. These papers concluded that cyclic MP performed worse than acyclic MP, but cyclic MP was more appropriate considering the practical challenges of implementation in real life.

Other papers also tried to solve problems related to connected and autonomous vehicles (CAV) (Rey and Levin, 2019; Cao et al., 2020; Zhang et al., 2020), autonomous intersection management (AIM) with pedestrians (Chen et al., 2020), AIM with dynamic lane reversal (Levin et al., 2019), cyber-attacks on traffic signals (Yen et al., 2018), vehicle routing (Taale et al., 2015; Gregoire et al., 2016; Liu et al., 2018), public transit signal priority (Xu et al., 2022), maximum stability dispatching policy (Li et al., 2021; Kang and Levin, 2021; Xu et al., 2021a) using similar analysis and proof techniques.

All of the papers mentioned so far, used MP control on all of the signalized intersections. The literature does not contain any proof of stability or numerical results with a limited deployment of MP control. The maximum servable demand may change with different number of MP controlled intersections. So, stability guarantees that work with all MP controlled intersections may not work for a limited number of MP controlled intersections. This is because not having MP control in some intersection can reduce the maximum servable demand of the network. Whether a network can still be stabilized with theoretical guarantees if only a limited number of intersection controls are allowed to be modified is not studied in the literature. This paper is the first one that attempts to tackle this problem.

3. Methodology

We represent the traffic network as a directed graph where the intersections are the nodes of the graph. Two types of nodes are considered: 1. Nodes where MP control is installed and 2. Nodes where the existing pretimed traffic signal is installed. Then we present the queuing model based on which the vehicle dynamics are determined. We use the point queue link model given by Vickrey (1963) with this queueing model. The point queue link model makes two assumptions about a link: 1. A link has a uncongestible physical section where vehicles can travel at freeflow speed and 2. A point queue at the downstream end of the link occupying no physical space where an infinite number of vehicles are allowed to stack up. The physical section represents the travel time on the link with no congestion and the point queue represents the delay due to congestion. Even though the point queue model does not completely capture traffic behavior, many previous papers (e.g. Varaiya, 2013; Le et al., 2015; Levin et al., 2019) used it to prove stability properties. This is mainly because with the point queue model it is easier to theoretically show that the network can still be stabilized. Barman and Levin (2022), Robbennolt et al. (2022) showed using simulations created based on real life traffic data that, even with this assumption the claimed performance guarantees from the theoretical models of MP controls can still be achieved. We define the limited deployment of MP control next. Then the stable region or the set of demands that can be stabilized for any signal control with limited budget to modify traffic signals is defined. We call that the stable region for limited deployment. Then we show that for all demand in the stable region limited deployment of MP control is stable, meaning the sum of the queue lengths for the network will be bounded over a long period. We also show that if demand is not in the stable region network cannot be stabilized by any signal control.

Consider a directed graph, $\mathcal{G} = (\mathcal{N}, \mathcal{A})$. The sets of all nodes and links are denoted by $\mathcal{N}$ and $\mathcal{A} = \mathcal{A}_{\mathrm{r}} \cup \mathcal{A}_{\mathrm{i}} \cup \mathcal{A}_{\mathrm{s}}$ respectively. Here, $\mathcal{A}_{\mathrm{r}}, \mathcal{A}_{\mathrm{i}}$ and $\mathcal{A}_{\mathrm{s}}$ are the sets of entry, internal and exit links respectively. $I(n)$ and $O(n)$ are the sets of incoming and outgoing links from node n respectively. $\mathcal{I}(i)$ and $\mathcal{O}(i)$ are the sets of incoming and outgoing links to and from link i respectively. The tuple (i, j) represents a movement from link i to link j. Define the set of allowed movement via node n to be $\mathcal{M}_n = \{(i, j)\ \forall i \in I(n)\ \forall j \in O(n)\}$.

Let $\mathcal{N}^{\pi} \subseteq \mathcal{N}$ be the set of nodes where MP is installed and the rest of the nodes be $\mathcal{N}^{\sigma} = \mathcal{N} \setminus \mathcal{N}^{\pi}$, the set of nodes controlled by some other control policy. In other words, nodes in $\mathcal{N}^{\sigma}$ have fixed traffic control that cannot be changed and nodes in $\mathcal{N}^{\pi}$ will be controlled using MP control. While $\mathcal{N}^{\pi} = \mathcal{N}$ meaning that all intersections are controlled with MP control is ideal, budget limitations may render it impractical. Furthermore, demand for some intersections may not be sufficiently large so that replacing the signal control with MP control would have any impactful practical benefit.

Before discussing traffic signal control policies, we define the queuing model to describe how vehicles will move around throughout the network.

$$x_{ij}(t+1) = x_{ij}(t) - y_{ij}(t) + d_i(t)P_{ij}(t) \qquad \forall i \in \mathcal{A}_{\mathrm{r}}\ \forall j \in \mathcal{O}(i) \tag{1}$$

$$x_{jk}(t+1) = x_{jk}(t) - y_{jk}(t) + \sum_{i \in \mathcal{I}(j)} y_{ij}(t)P_{jk}(t) \qquad \forall j \in \mathcal{A}_{\mathrm{i}}\ \forall k \in \mathcal{O}(j) \tag{2}$$

$$y_{ij}(t) = \min\left\{Q_{ij}S_{ij}(t),\ x_{ij}(t)\right\} \qquad \forall n \in N\ \forall (i,j) \in \mathcal{M}_n \tag{3}$$

where $d_i(t)$ and $P_{ij}(t)$ are the exogenous demand coming into link i and turning proportions for movement (i,j) at time t respectively. $Q_{ij}(t)$ represents the saturation rate and $S_{ij}(t) \in \{0,1\}$ represents whether the movement is inactive or active for the movement (i,j) at time t. Here Eqs. (1) and (2) indicate that the queue length at the next time step is equal to the queue length minus the leaving vehicles plus the entering vehicles at the current time step. At most the vehicles present at the queue $x_{ij}(t)$ can leave the queue. Vehicles are allowed to leave the queue only if the signal is active or $S_{ij}(t) = 1$. $y_{ij}(t)$ is the flow that is allowed to move at time step t and is determined by the minimum of the queue length and saturation rate if signal is active.

The queuing process $\{\mathbf{x}(t) : t \geq 0\}$ where, $\mathbf{x}(t) = \left\{x_{ij}(t)\ \forall n \in N\ \forall (i,j) \in \mathcal{M}_n\right\}$ depends on the signal control policy $\phi : \mathbf{x}(t) \to S(t)$ and independent and identically distributed (iid) random vector $\mathbf{d}(t)$ and matrix $P(t)$. The demand vector $\mathbf{d}(t)$ at time t is a vector of random variables that represents the number of vehicles entering the network for all entry links at time t. The matrix $P(t)$ describes the constant historical turn proportions for all movements in the network. Both $\mathbf{d}(t)$ and $P(t)$ are independent of the previous states $x(t), \ldots, x(1)$ of the system. Therefore, the next state only depends on the current state and some iid random variable $h(\cdot)$ using the control ϕ. Therefore, the queuing process can be written as

$$\mathbf{x}(t+1) = g_{\phi}(\mathbf{x}(t), h(\mathbf{d(t)}, P(t))) \tag{4}$$

Again, since $\mathbf{d}(t)$, $P(t)$ are iid random variables and the function $h(\cdot)$ maps to iid random variables, the queuing model is a Markov chain using the control ϕ. This allows us to use different Markovian properties for our analysis in the next section.

Varaiya (2013) showed that routing and flow conservation are described by the following equations.

$$f_i(t) = d_i(t) \qquad \forall i \in \mathcal{A}_{\mathrm{r}} \tag{5}$$

$$f_j(t) = \sum_{i \in \mathcal{I}(j)} f_i(t)P_{ij}(t) \qquad \forall j \in \mathcal{A}_{\mathrm{i}} \cup \mathcal{A}_{\mathrm{s}} \tag{6}$$

Here the flow on the entry links is exactly equal to the exogenous demands and flow for other links are determined by turn proportions and flow conservation at each node. Varaiya (2013) also showed the following.

Proposition 1. *For every demand vector* $\mathbf{d} = \left\{d_i\ \forall i \in \mathcal{A}_{\mathrm{r}}\right\}$ *there is a unique flow* $\mathbf{f} = \left\{f_i\ \forall i \in \mathcal{A}\right\}$ *satisfying Eqs.* (5) and (6). *Hence, there is a matrix* P*, which depends only on the turn proportions, such that* $\mathbf{f} = \mathbf{d}P$.

3.1. Limited deployment

Define the MP control, some other control and the limited deployment control policies with π, σ and μ respectively. Let $S^{\pi}_{ij}(t)$ and $S^{\sigma}_{ij}(t)$ indicate whether signal is active for nodes in $\mathcal{N}^{\pi}$ and nodes in $\mathcal{N}^{\sigma}$ respectively for movement (i,j) at time t. At node n, time t signal activation for movement (i,j) with limited deployment policy μ is defined as the following

$$S^{\mu}_{ij}(t) = \begin{cases} S^{\pi}_{ij}(t) & \text{if } n \in \mathcal{N}^{\pi} \\ S^{\sigma}_{ij}(t) & \text{if } n \in \mathcal{N}^{\sigma} \end{cases} \tag{7}$$

A network control matrix $S(t) = [[S_{ij}(t)\ \forall j \in A]\forall i \in A]$ describes the signal activation status for all movements of the network at time t. With limited deployment of max pressure controllers, an intersection control matrix $S_n(t) = [[S_{ij}(t)\ \forall j \in O(n)]\forall i \in I(n)]$ depends on the type of signal control that is installed at the intersection. Varaiya (2013) discusses these matrices in greater detail. Let $\mathcal{S}$ and $\mathcal{S}_n$ be the sets of all feasible network and intersection control matrices, and define the convex hull of $\mathcal{S}$ as

$$\mathrm{co}(\mathcal{S}) = \left\{ \sum_{S \in \mathcal{S}} \lambda_S S \;\middle|\; \sum_{S \in \mathcal{S}} \lambda_S = 1, \lambda_S \geq 0 \right\} \tag{8}$$

where the fraction of activation time λ_S is given to each intersection control matrix $S \in \mathcal{S}$. We will use this definition of convex hull in the next section while analyzing the stable region and in the description of MP control.

The intersection control matrix using max pressure at time t can be obtained by solving the optimization problem (9) for all nodes in $\mathcal{N}^{\pi}$,

$$S^{\pi}_n(t) = \arg\max_{S \in \mathrm{co}(\mathcal{S}_n)} \left\{ \sum_{(i,j) \in \mathcal{M}_n} Q_{ij}S_{ij}w_{ij}(t) \right\} \tag{9}$$

with $w_{ij}(t)$ defined by

$$w_{ij}(t) = x_{ij}(t) - \sum_{k\in\mathcal{O}(j)} x_{jk}(t)\bar{P}_{jk} \tag{10}$$

here for each movement (i,j) a weight $w_{ij}(t)$ is defined. MP control defines a pressure term for each combination of movements called a phase. The pressure term is the weighted sum of all the vehicles that are allowed to move during a phase. Here, MP control selects the network control matrix for which the total pressure for all movement is maximized. Varaiya (2013) showed that choosing a phase by maximizing this pressure term with the weight function defined in Eq. (10) results in a signal control that can stabilize a network with stabilizable demand.

Assume that the sequence of intersection control matrices $\{S_n^\sigma(t)\}_{t=1}^{C}$ with cycle length C is given. After every C timesteps the intersection control matrix at the beginning of that sequence is activated and then the rest of the sequence are followed in order. This other traffic signal controller can be the already existing traffic signal controller. For all nodes $n \in \mathcal{N}^\sigma$ this other signal control should select the intersection control matrix $S_n^\sigma(t)$ at time t.

Lemma 1. *The average network control matrix of some signal control policy $\phi : x(t) \to S(t)$ is defined by*

$$\mathbb{S} = \lim_{T\to\infty} \frac{1}{T} \sum_{t=1}^{T} \phi(\mathbf{x}(t)) \tag{11}$$

and

$$\mathbb{S} \in \mathrm{co}(\mathcal{S}) \tag{12}$$

Proof. The Markov chain $\mathbf{x}(t)$ is a function of i.i.d. random demand vector $\mathbf{d}(t)$ and random turn proportions matrix $P(t)$. All previous work with stability proofs made the same i.i.d. assumption. The network signal control matrix $\phi(\cdot)$ is a function of $\mathbf{x}(t)$ and over a long period $\mathbf{x}(t)$ is identically distributed over time. Therefore, we assume that $\phi(\cdot)$ is identically distributed over time as well. Over a long period of time, the proportion of time spent in each phase should converge to the average. If those average proportions of time in each phase are known, then the following limit will exist.

$$\mathbb{E}\{\phi(\mathbf{x}(t))\} = \mathbb{S} = \lim_{T\to\infty} \frac{1}{T} \sum_{t=1}^{T} \phi(\mathbf{x}(t)) \tag{13}$$

Assume that over the time period T, the signal control matrices $S_1, S_2, \dots, S_m$ were activated for $a_1, a_2, \dots, a_m$ times respectively. Now Eq. (11) can be rewritten as

$$\mathbb{S} = \frac{\sum_{j=1}^{m} a_j S_j}{\sum_{i=1}^{m} a_i} = \frac{a_1 S_1}{\sum_{i=1}^{m} a_i} + \frac{a_2 S_2}{\sum_{i=1}^{m} a_i} + \cdots + \frac{a_m S_m}{\sum_{i=1}^{m} a_i} \tag{14}$$

since $a_j \geq 0$ is the number of times network control matrix S_j was activated and $a_j \leq \sum_{i=1}^{m} a_i$ for all $j \in \{1,\dots,m\}$. Therefore, over total T time period the fraction of time λ_{S_j} signal control matrix S_j was activated is

$$\lambda_{S_j} = \frac{a_j}{\sum_{i=1}^{m} a_i} \geq 0 \qquad \forall j \in \{1,\dots,m\} \tag{15}$$

and clearly, $\sum_{S\in\mathcal{S}} \lambda_S = \sum_{j=1}^{m} \frac{a_j}{\sum_{i=1}^{m} a_i} = 1$. So, $\mathbb{S} \in \mathrm{co}(\mathcal{S})$. $\square$

3.2. Stable region for limited deployment

We define the stable region to be the set of all demands that can be stabilized by some signal control. It is created by converting the average demand vector $\bar{\mathbf{d}}$ using the turning proportions matrix $\bar{P}$ to average link flow vector $\bar{\mathbf{f}}$ and then checking whether a signal control can serve those demands on average. Define the feasible demands for the MP control by

$$\mathcal{D}_\pi^\circ = \left\{\mathbf{d} : (\bar{\mathbf{f}} = \bar{\mathbf{d}}\bar{P}) \wedge (\exists \mathbb{S} \in \mathrm{co}(\mathcal{S}) \text{ s.t. } \mathbb{S}_{ij}Q_{ij} > \bar{f}_i\bar{P}_{ij}\ \forall n \in \mathcal{N}^\pi, \forall (i,j) \in \mathcal{M}_n)\right\} \tag{16}$$

where the average network control matrix $\mathbb{S} \in \mathrm{co}(\mathcal{S})$. This is proven in Lemma 1. Let the feasible demands for some other controller with average signal activation $\bar{S}^\sigma$ represented by

$$\mathcal{D}_\sigma^\circ = \left\{\mathbf{d} : (\bar{\mathbf{f}} = \bar{\mathbf{d}}\bar{P}) \wedge (\bar{S}_{ij}^\sigma Q_{ij} > \bar{f}_i\bar{P}_{ij}\ \forall n \in \mathcal{N}^\sigma, \forall (i,j) \in \mathcal{M}_n)\right\} \tag{17}$$

Now we only allow modifying the control on nodes in $\mathcal{N}^\pi$ and keep the controls on nodes in $\mathcal{N}^\sigma$ unchanged. With this consideration the feasible demands for limited deployment can be defined as

$$\mathcal{D}_\mu^\circ = \left\{\mathbf{d} : (\bar{\mathbf{f}} = \bar{\mathbf{d}}\bar{P})\ \wedge\ \left(\exists \mathbb{S} \in \mathrm{co}(\mathcal{S}) \text{ s.t. } \mathbb{S}_{ij}Q_{ij} > \bar{f}_i\bar{P}_{ij}\ \forall n \in \mathcal{N}^\pi, \forall (i,j) \in \mathcal{M}_n\ \ \wedge\ \ \bar{S}_{ij}^\sigma Q_{ij} > \bar{f}_i\bar{P}_{ij}\ \forall n \in \mathcal{N}^\sigma, \forall (i,j) \in \mathcal{M}_n\right)\right\} \tag{18}$$

Therefore, $\mathcal{D}_\mu^\circ \subseteq \mathcal{D}_\pi^\circ$. We will show that if the average demand vector is in the stable region then limited deployment can stabilize the network. Otherwise, no signal controller can stabilize the network.

3.3. Stability with limited deployment

Before analyzing the stability of limited deployment, we first define what stability means in Definition 1. If the average queue length for the entire network is bounded by some constant $K < \infty$ then the network is said to be stable. Using the bound K we will further show that the average length of individual queues will also be bounded. Like Varaiya (2013) we will show that this bound does not depend on the network and only depends on the maximum values of demand and saturation rates.

Definition 1. A network is stable if under average demand $\bar{\mathbf{d}}$, there exists a constant $K < \infty$ such that

$$\lim_{T\to\infty} \mathbb{E}\left\{\frac{1}{T}\sum_{t=1}^{T}\sum_{(i,j)\in\mathcal{A}^2} x_{ij}(t)\right\} < K \tag{19}$$

This definition of stability ensures that the total average queue length over a large period of time will be bounded. The total average queue length can only be bounded if each individual queue is also bounded on average. Each individual queue can be bounded if on average, service rate exceeds demand on each individual queue. We will show in Theorem 2 that if average demand vector $\bar{\mathbf{d}}$ is in the stable region $\mathcal{D}_\mu^\circ$ then with limited deployment control the network can be stabilized. Otherwise, if $\bar{\mathbf{d}}$ is not in the stable region $\mathcal{D}_\mu^\circ$ then there exists no control that can stabilize the network. That means limited deployment control can stabilize all possibly stabilizable demands and the only demands that it cannot stabilize, cannot be stabilized by any other control. That is referred to as the maximum stability property in the literature since it means that the control can stabilize the network for all possibly stabilizable demands.

Lemmas 2, 3 and the respective proofs will be presented here before using them in Theorem 2. To prove Lemma 2 we will use an established result given in Theorem 1 (Hoffman and Kruskal, 2016). Properties of totally unimodular matrices are used in Theorem 1. So, we give the definition of totally unimodular matrices in Definition 2 before stating Theorem 1.

Definition 2. Matrix $A \in \mathbb{R}^{m\times n}$ is totally unimodular (TU) if $\det(\mathrm{SS}_i(A)) \in \{-1, 0, +1\}$ for all i where, SS_i is the ith square submatrix of A.

Theorem 1 (*Hoffman–Kruskal Theorem (Hoffman and Kruskal, 2016)*). *If A is TU and b is an integer vector then, polytope $P = \{x : Ax \le b\}$ has only integer vertices.*

Lemma 2.

$$\max_{S\in\mathcal{S}}\left\{\sum_{(i,j)\in\mathcal{M}_n} S_{ij}Q_{ij}w_{ij}(t)\right\} = \max_{\mathbb{S}\in\mathrm{co}(\mathcal{S})}\left\{\sum_{(i,j)\in\mathcal{M}_n} \mathbb{S}_{ij}Q_{ij}w_{ij}(t)\right\} \qquad \forall n \in \mathcal{N}^\pi \tag{20}$$

Proof. The convex hull can be written as

$$\mathrm{co}(\mathcal{S}) = \left\{\sum_{S\in\mathcal{S}} \lambda_S S \;\middle|\; A^T\lambda = \mathbf{b}, \lambda_S \ge 0\ \forall S \in \mathcal{S}\right\} \tag{21}$$

where

$$A = \begin{bmatrix}1\\1\\\vdots\\1\end{bmatrix} \in \mathbb{R}^{|\mathcal{S}|\times 1} \qquad \lambda = \begin{bmatrix}\lambda_1\\\lambda_2\\\vdots\\\lambda_{|\mathcal{S}|}\end{bmatrix} \in \mathbb{R}^{|\mathcal{S}|\times 1} \qquad b = 1 \tag{22}$$

Here, $\det(\mathrm{SS}_i(A)) = 1 \in \{-1, 0, +1\}$. According to Theorem 1 A is TU and $b = 1$ is integer. So, the polytope $\mathrm{co}(\mathcal{S})$ only has integer vertices or extreme points.

According to the Linear Programming (LP) Fundamental Theorem (Chong and Zak, 2004), if there is an optimal solution then there is an optimal solution that is a basic feasible solution (BFS). For a standard LP polytope $\{\lambda : A^T\lambda = \mathbf{b}, \lambda \ge 0\}$, λ is a BFS if and only if λ is an extreme point. Since, all BFS's in the polytope $\mathrm{co}(\mathcal{S})$ are integers there exists an optimal solution with entries $\mathbb{S}_{ij}$ in $\{0, 1\}$ for all $(i,j) \in \mathcal{M}_n$ for all $n \in \mathcal{N}$. □

Define the max pressure policy by $\pi : \mathbf{x}_n(t) \to S_n^\pi(t)$, some other signal control policy $\sigma : \mathbf{x}_n(t) \to S_n^\sigma(t)$. Now the limited deployment policy can be defined by $\mu : \mathbf{x}_n(t) \to S_n^\mu(t)$.

Lemma 3.

$$\alpha_1 = \sum_{i\in\mathcal{A}_r}\sum_{j\in\mathcal{O}(i)} w_{ij}(t)\left[\bar{f}_i\bar{P}_{ij} - Q_{ij}\bar{S}_{ij}^\mu\right] \le -\epsilon\eta\|\mathbf{x}(t)\| \tag{23}$$

Proof. Since π maximizes pressure, any other controller σ cannot result in more pressure from the signal.

$$\sum_{n\in N}\sum_{(i,j)\in\mathcal{M}_n} S^{\pi}_{ij}(t)Q_{ij}w_{ij}(t) \geq \sum_{n\in N}\sum_{(i,j)\in\mathcal{M}_n} S^{\sigma}_{ij}(t)Q_{ij}w_{ij}(t) \tag{24}$$

With limited deployment, MP only controls nodes where MP is installed and on other nodes we assume the signal timing is exogenous represented by S^{σ}.

$$\sum_{n\in\mathcal{N}}\sum_{(i,j)\in\mathcal{M}_n} S^{\mu}_{ij}(t)Q_{ij}w_{ij}(t) = \sum_{n\in\mathcal{N}^{\pi}}\sum_{(i,j)\in\mathcal{M}_n} S^{\pi}_{ij}(t)Q_{ij}w_{ij}(t) + \sum_{n\in\mathcal{N}^{\sigma}}\sum_{(i,j)\in\mathcal{M}_n} S^{\sigma}_{ij}(t)Q_{ij}w_{ij}(t) \tag{25}$$

Therefore,

$$\sum_{n\in\mathcal{N}}\sum_{(i,j)\in\mathcal{M}_n} S^{\pi}_{ij}(t)Q_{ij}w_{ij}(t) \geq \sum_{n\in\mathcal{N}}\sum_{(i,j)\in\mathcal{M}_n} S^{\mu}_{ij}(t)Q_{ij}w_{ij}(t) \geq \sum_{n\in\mathcal{N}}\sum_{(i,j)\in\mathcal{M}_n} S^{\sigma}_{ij}(t)Q_{ij}w_{ij}(t) \tag{26}$$

Now by Lemma 2 and the definition of MP control, when $\mathcal{N}^{\pi}=\mathcal{N}$

$$\sum_{(i,j)\in\mathcal{M}_n} S^{\pi}_{ij}(t)Q_{ij}w_{ij}(t) = \max_{S\in\mathcal{S}}\left\{\sum_{(i,j)\in\mathcal{M}_n} Q_{ij}S_{ij}w_{ij}(t)\right\} = \max_{\mathbb{S}\in\mathrm{co}(\mathcal{S})}\left\{\sum_{(i,j)\in\mathcal{M}_n} Q_{ij}\mathbb{S}_{ij}w_{ij}(t)\right\} \tag{27}$$

By Eqs. (25) and (27)

$$\sum_{n\in\mathcal{N}}\sum_{(i,j)\in\mathcal{M}_n} S^{\mu}_{ij}(t)Q_{ij}w_{ij}(t) = \max_{\mathbb{S}\in\mathrm{co}(\mathcal{S})}\left\{\sum_{(i,j)\in\mathcal{M}_n} Q_{ij}\mathbb{S}_{ij}w_{ij}(t)\right\} + \sum_{n\in\mathcal{N}^{\sigma}}\sum_{(i,j)\in\mathcal{M}_n} S^{\sigma}_{ij}(t)Q_{ij}w_{ij}(t) \tag{28}$$

When $d\in D^{\circ}_{\mu}$ then for all $n\in\mathcal{N}^{\pi}$ there exists $\mathbb{S}\in\mathrm{co}(\mathcal{S})$ such that

$$\mathbb{S}_{ij}Q_{ij} = \begin{cases}\bar{f}_i\bar{P}_{ij}+\epsilon & \text{if } w_{ij}(t)>0\\ 0 & \text{if } w_{ij}(t)\leq 0\end{cases} \qquad \bar{S}^{\sigma}_{ij}Q_{ij} = \begin{cases}\bar{f}_i\bar{P}_{ij}+\epsilon & \text{if } w_{ij}(t)>0\\ 0 & \text{if } w_{ij}(t)\leq 0\end{cases}$$

here $\bar{S}^{\sigma}$ is the average exogenous signal control.

$$\alpha_1 = \sum_{n\in\mathcal{N}}\sum_{(i,j)\in\mathcal{M}_n}\left[\bar{f}_i\bar{P}_{ij}-\bar{S}^{\mu}_{ij}Q_{ij}\right]w_{ij}(t) \tag{29}$$

$$= \sum_{n\in\mathcal{N}^{\pi}}\sum_{(i,j)\in\mathcal{M}_n}\left[\bar{f}_i\bar{P}_{ij}-\mathbb{S}_{ij}Q_{ij}\right]w_{ij}(t) + \sum_{n\in\mathcal{N}^{\sigma}}\sum_{(i,j)\in\mathcal{M}_n}\left[\bar{f}_i\bar{P}_{ij}-\bar{S}^{\sigma}_{ij}Q_{ij}\right]w_{ij}(t) \tag{30}$$

$$= \sum_{n\in\mathcal{N}^{\pi}}\sum_{(i,j)\in\mathcal{M}_n}\left[-\epsilon w_{ij}(t)^{+}+\bar{f}_i\bar{P}_{ij}w_{ij}(t)^{-}\right] + \sum_{n\in\mathcal{N}^{\sigma}}\sum_{(i,j)\in\mathcal{M}_n}\left[-\epsilon w_{ij}(t)^{+}+\bar{f}_i\bar{P}_{ij}w_{ij}(t)^{-}\right] \tag{31}$$

$$= \sum_{n\in\mathcal{N}}\sum_{(i,j)\in\mathcal{M}_n}\left[-\epsilon w_{ij}(t)^{+}+\bar{f}_i\bar{P}_{ij}w_{ij}(t)^{-}\right] \;\leq\; -\epsilon\sum_{n\in N}\sum_{(i,j)\in\mathcal{M}_n}|w_{ij}(t)| \tag{32}$$

According to Varaiya (2013) since the map $w:\mathbf{x}\to\mathbb{R}$ is injective there exists $\eta>0$ such that

$$\sum_{n\in N}\sum_{(i,j)\in\mathcal{M}_n}|w_{ij}(t)| \geq \eta\|\mathbf{x}(t)\| \tag{33}$$

Therefore, $\alpha_1\leq -\epsilon\eta\|\mathbf{x}(t)\|$ □

Theorem 2. *Under the limited deployment of MP control policy $\mu:\mathbf{x}(t)\to S(t)$, the network is stable as per Definition 1 for average demand vector $\bar{\mathbf{d}}\in\mathcal{D}^{\circ}_{\mu}$, $\mathbb{E}|x(1)|$ is bounded and the exogenous traffic signal control is stable according to Definition 1.*

Proof. Define the Lyapunov function $V:\mathbf{x}(t)\to\|\mathbf{x}(t)\|^2$ which maps the queue length vector to the sum of square of the queue lengths. The Lyapunov drift can be written as,

$$\Delta V(\mathbf{x}) = \mathbb{E}\left\{V(\mathbf{x}(t+1))-V(\mathbf{x}(t))\,\middle|\,\mathbf{x}(t)\right\} = \mathbb{E}\left\{\|\mathbf{x}(t+1)\|^2-\|\mathbf{x}(t)\|^2\,\middle|\,\mathbf{x}(t)\right\} \tag{34}$$

Define $\boldsymbol{\delta}=\mathbf{x}(t+1)-\mathbf{x}(t)$.

$$\delta_{ij} = x_{ij}(t+1)-x_{ij}(t) = -y_{ij}(t)+d_i(t)P_{ij}(t) \qquad \forall i\in\mathcal{A}_{\mathrm{r}}\ \forall j\in\mathcal{O}(i) \tag{35}$$

$$\delta_{jk} = x_{jk}(t+1)-x_{jk}(t) = -y_{jk}(t)+\sum_{i\in\mathcal{I}(j)}y_{ij}(t)P_{jk}(t) \qquad \forall j\in\mathcal{A}_{\mathrm{i}}\cup\mathcal{A}_{\mathrm{s}}\ \forall k\in\mathcal{O}(j) \tag{36}$$

Now, the difference of the Lyapunov functions with inputs $x(t+1)$ and $x(t)$ can be written as

$$\|\mathbf{x}(t+1)\|^2-\|\mathbf{x}(t)\|^2 = \|\mathbf{x}(t)+\delta\|^2-\|\mathbf{x}(t)\|^2 = 2\mathbf{x}(t)^T\boldsymbol{\delta}+\|\boldsymbol{\delta}\|^2 \tag{37}$$

Taking the expected value conditioned on $\mathbf{x}(t)$

$$\Delta V(\mathbf{x}) = \mathbb{E}\left\{\|\mathbf{x}(t+1)\|^2-\|\mathbf{x}(t)\|^2 \mid \mathbf{x}(t)\right\} = 2\mathbb{E}\left\{\mathbf{x}(t)^T\boldsymbol{\delta}\mid\mathbf{x}(t)\right\}+\mathbb{E}\left\{\|\boldsymbol{\delta}\|^2\mid\mathbf{x}(t)\right\} \tag{38}$$

Here

$$x(t)^T\delta = \sum_{i\in\mathcal{A}_r}\sum_{j\in\mathcal{O}(i)} x_{ij}(t)\left[-y_{ij}(t)+d_i(t)P_{ij}(t)\right] + \sum_{j\in\mathcal{A}_i}\sum_{k\in\mathcal{O}(j)} x_{jk}(t)\left[-y_{jk}(t)+\sum_{i\in\mathcal{I}(j)} y_{ij}(t)P_{jk}(t)\right] \tag{39}$$

$$= \sum_{i\in\mathcal{A}_r}\sum_{j\in\mathcal{O}(i)} d_i(t)P_{ij}(t)x_{ij}(t) + \sum_{j\in\mathcal{A}_r\cup\mathcal{A}_i}\sum_{k\in\mathcal{O}(j)} x_{jk}(t)(-y_{jk}(t)) + \sum_{j\in\mathcal{A}_i}\sum_{k\in\mathcal{O}(j)} x_{jk}(t)\sum_{i\in\mathcal{I}(j)} y_{ij}(t)P_{jk}(t) \tag{40}$$

$$= \sum_{i\in\mathcal{A}_r}\sum_{j\in\mathcal{O}(i)} d_i(t)P_{ij}(t)x_{ij}(t) + \sum_{i\in\mathcal{A}_r\cup\mathcal{A}_i}\sum_{j\in\mathcal{O}(i)} y_{ij}(t)\left(-x_{ij}(t)+\sum_{k\in\mathcal{O}(j)} x_{jk}(t)P_{jk}(t)\right) \tag{41}$$

Since $P_{ij}(t)$ is independent of $y_{ij}(t)$ and $\mathbf{x}(t)$, by the law of total expectation we get

$$\mathbb{E}\left\{y_{ij}(t)P_{jk}(t)x_{jk}(t)\mid \mathbf{x}(t)\right\} = \mathbb{E}\left\{\mathbb{E}\left\{y_{ij}(t)P_{jk}(t)x_{jk}(t)\mid y_{ij}(t),\mathbf{x}(t)\right\}\ \mid \mathbf{x}(t)\right\} = \mathbb{E}\left\{y_{ij}(t)\mid \mathbf{x}(t)\right\}\bar{P}_{jk}x_{jk}(t) \tag{42}$$

Taking the expectation of $\mathbf{x}(t)^T\delta$ conditioned on $\mathbf{x}(t)$ we get

$$\mathbb{E}\left\{\mathbf{x}(t)^T\delta \,\middle|\, \mathbf{x}(t)\right\} = \mathbb{E}\left\{\sum_{i\in\mathcal{A}_r} d_i(t)P_{ij}(t)x_{ij}(t) + \sum_{i\in\mathcal{A}_r\cup\mathcal{A}_i}\sum_{j\in\mathcal{O}(i)} y_{ij}(t)\left[-x_{ij}(t)+\sum_{k\in\mathcal{O}(j)} x_{jk}(t)P_{jk}(t)\right] \,\middle|\, \mathbf{x}(t)\right\} \tag{43}$$

$$=\mathbb{E}\left\{\sum_{i\in\mathcal{A}_r} d_i(t)P_{ij}(t)x_{ij}(t)\mid \mathbf{x}(t)\right\} + \mathbb{E}\left\{\sum_{i\in\mathcal{A}_r\cup\mathcal{A}_i}\sum_{j\in\mathcal{O}(i)} y_{ij}(t)\left[-x_{ij}(t)+\sum_{k\in\mathcal{O}(j)} x_{jk}(t)P_{jk}(t)\right] \,\middle|\, \mathbf{x}(t)\right\} \tag{44}$$

$$= \sum_{i\in\mathcal{A}_r} \bar{d}_i\bar{P}_{ij}x_{ij}(t) + \sum_{i\in\mathcal{A}_r\cup\mathcal{A}_i}\sum_{j\in\mathcal{O}(i)} \mathbb{E}\left\{y_{ij}(t)\mid \mathbf{x}(t)\right\}\left[-x_{ij}(t)+\sum_{k\in\mathcal{O}(j)} x_{jk}(t)\bar{P}_{jk}\right] \tag{45}$$

$$= \sum_{i\in\mathcal{A}_r} \bar{d}_i\bar{P}_{ij}x_{ij}(t) - \sum_{i\in\mathcal{A}_r\cup\mathcal{A}_i}\sum_{j\in\mathcal{O}(i)} \mathbb{E}\left\{y_{ij}(t)\mid \mathbf{x}(t)\right\} w_{ij}(t) \tag{46}$$

Now,

$$\sum_{i\in\mathcal{A}_r\cup\mathcal{A}_i}\sum_{j\in\mathcal{O}(i)} f_i\bar{P}_{ij}w_{ij}(t) = \sum_{i\in\mathcal{A}_r\cup\mathcal{A}_i}\sum_{j\in\mathcal{O}(i)} f_i\bar{P}_{ij}\left[x_{ij}(t)-\sum_{k\in\mathcal{O}(j)} x_{jk}(t)\bar{P}_{jk}\right] \tag{47}$$

$$= \sum_{i\in\mathcal{A}_r\cup\mathcal{A}_i}\sum_{j\in\mathcal{O}(i)} f_i\bar{P}_{ij}x_{ij}(t) - \sum_{i\in\mathcal{A}_r\cup\mathcal{A}_i}\sum_{j\in\mathcal{O}(i)} f_i\bar{P}_{ij}\left[\sum_{k\in\mathcal{O}(j)} x_{jk}(t)\bar{P}_{jk}\right] \tag{48}$$

$$= \sum_{i\in\mathcal{A}_r\cup\mathcal{A}_i}\sum_{j\in\mathcal{O}(i)} f_i\bar{P}_{ij}x_{ij}(t) - \sum_{j\in\mathcal{A}_i}\left[\sum_{i\in\mathcal{I}(i)} f_i\bar{P}_{ij}\right]\sum_{k\in\mathcal{O}(j)} x_{jk}(t)\bar{P}_{jk} \tag{49}$$

$$= \sum_{i\in\mathcal{A}_r\cup\mathcal{A}_i}\sum_{j\in\mathcal{O}(i)} f_i\bar{P}_{ij}x_{ij}(t) - \sum_{j\in\mathcal{A}_i} f_j\sum_{k\in\mathcal{O}(j)} x_{jk}(t)\bar{P}_{jk} \tag{50}$$

$$= \sum_{i\in\mathcal{A}_r}\sum_{j\in\mathcal{O}(i)} f_i\bar{P}_{ij}x_{ij}(t) = \sum_{i\in\mathcal{A}_r}\sum_{j\in\mathcal{O}(i)} \bar{d}_i\bar{P}_{ij}x_{ij}(t) \tag{51}$$

Eqs. (46) and (51) give

$$\mathbb{E}\left\{\mathbf{x}(t)^T\delta\mid \mathbf{x}(t)\right\} = \sum_{i\in\mathcal{A}_r} \bar{d}_i\bar{P}_{ij}x_{ij}(t) - \sum_{i\in\mathcal{A}_r\cup\mathcal{A}_i}\sum_{j\in\mathcal{O}(i)} \mathbb{E}\left\{y_{ij}(t)\mid \mathbf{x}(t)\right\} w_{ij}(t) \tag{52}$$

$$= \sum_{i\in\mathcal{A}_r\cup\mathcal{A}_i}\sum_{j\in\mathcal{O}(i)} f_i\bar{P}_{ij}w_{ij}(t) - \sum_{i\in\mathcal{A}_r\cup\mathcal{A}_i}\sum_{j\in\mathcal{O}(i)} \mathbb{E}\left\{y_{ij}(t)\mid \mathbf{x}(t)\right\} w_{ij}(t) \tag{53}$$

$$= \sum_{i\in\mathcal{A}_r}\sum_{j\in\mathcal{O}(i)} w_{ij}(t)\left[\bar{f}_i\bar{P}_{ij} - Q_{ij}\bar{S}^{\mu}_{ij} + Q_{ij}\bar{S}^{\mu}_{ij} - \mathbb{E}\left\{y_{ij}(t)\mid \mathbf{x}(t)\right\}\right] \tag{54}$$

$$=\alpha_1+\alpha_2 \tag{55}$$

where

$$\alpha_1 = \sum_{i\in\mathcal{A}_r}\sum_{j\in\mathcal{O}(i)} w_{ij}(t)\left[\bar{f}_i\bar{P}_{ij} - Q_{ij}\bar{S}^{\mu}_{ij}\right] \tag{56}$$

$$\alpha_2 = \sum_{i\in\mathcal{A}_r}\sum_{j\in\mathcal{O}(i)} w_{ij}(t)\left[Q_{ij}\bar{S}^{\mu}_{ij} - \mathbb{E}\left\{y_{ij}(t)\mid \mathbf{x}(t)\right\}\right] \tag{57}$$

Since $S^{\mu}_{ij}(t)\in\{0,1\}$, the second term in Eq. (57) can be bounded.

$$\mathbb{E}\left\{y_{ij}(t)\mid \mathbf{x}(t)\right\} = \mathbb{E}\left\{\min\left\{Q_{ij}S^{\mu}_{ij}(t), x_{ij}(t)\right\}\ \mid \mathbf{x}(t)\right\} \le Q_{ij} \tag{58}$$

and since $w_{ij}(t)\le x_{ij}(t)$, α_2 is bounded and the bound is a constant Mk_1 where, $M = |\cup_{n\in N}\mathcal{M}_n|$ is the total number of queues.

$$\alpha_1+\alpha_2 \le -\epsilon\eta\|\mathbf{x}(t)\| + Mk_1 \tag{59}$$

Varaiya (2013) showed that $\mathbb{E}\{\beta \mid \mathbf{x}(t)\} = \mathbb{E}\left\{\|\delta\|^2 \mid \mathbf{x}(t)\right\}$ is bounded by Mk_2^2 where, k_2 depends on the saturation rates and the maximum values of the demands.

$$\Delta V(\mathbf{x}) = \mathbb{E}\left\{ \|\mathbf{x}(t+1)\|^2 - \|\mathbf{x}(t)\|^2 \;\middle|\; \mathbf{x}(t)\right\} \le -\epsilon\eta\|\mathbf{x}(t)\| + Mk_1 + Mk_2^2 \tag{60}$$

Taking the unconditional expectation we get

$$\mathbb{E}\left\{\|\mathbf{x}(t+1)\|^2\right\} - \mathbb{E}\left\{\|\mathbf{x}(t)\|^2\right\} \le K - \epsilon\eta\mathbb{E}\|\mathbf{x}(t)\| \tag{61}$$

Summing from $t = 1$ to $t = T$

$$\sum_{t=1}^{T} K - \epsilon\eta \sum_{t=1}^{T} \mathbb{E}\|\mathbf{x}(t)\| \ge \sum_{t=1}^{T} \left(\mathbb{E}\|\mathbf{x}(t+1)\|^2 - \mathbb{E}\|\mathbf{x}(t)\|^2\right) \tag{62}$$

$$\begin{aligned} \implies KT - \epsilon\eta \sum_{t=1}^{T} \mathbb{E}\|\mathbf{x}(t)\| \ge\; & \mathbb{E}\|\mathbf{x}(2)\|^2 + \mathbb{E}\|\mathbf{x}(3)\|^2 + \cdots + \mathbb{E}\|\mathbf{x}(T)\|^2 + \mathbb{E}\|\mathbf{x}(T+1)\|^2 \\ & - \left(\mathbb{E}\|\mathbf{x}(1)\|^2 + \mathbb{E}\|\mathbf{x}(2)\|^2 + \cdots + \mathbb{E}\|\mathbf{x}(T)\|^2\right) \end{aligned} \tag{63}$$

$$\implies \epsilon\eta \frac{1}{T} \sum_{t=1}^{T} \mathbb{E}\|\mathbf{x}(t)\| \le K + \frac{1}{T}\mathbb{E}\|\mathbf{x}(1)\|^2 - \frac{1}{T}\mathbb{E}\|\mathbf{x}(T+1)\|^2 \le K + \frac{1}{T}\mathbb{E}\|\mathbf{x}(1)\|^2 \tag{64}$$

We assume that the initial state is uncongested or the queue lengths at time $t = 1$ is bounded which implies $\mathbb{E}|x(1)|$ is bounded. This assumption is reasonable: the number of vehicles initially in the network is some number and is therefore finite. The issue with $x(t)$ going to infinity occurs when $x(t)$ can increase over time as t goes to infinity. Since $\eta > 0$, Eq. (64) can be written as

$$\epsilon \frac{1}{T} \sum_{t=1}^{T} \mathbb{E}\|\mathbf{x}(t)\| \le \frac{1}{\eta}\left(K + \frac{1}{T}\mathbb{E}\|\mathbf{x}(1)\|^2\right) \tag{65}$$

which implies stability as per Definition 1. □

Theorem 2 proves that under limited deployment of MP controls, average queue length over long run will be bounded if $\bar{\mathbf{d}} \in \mathcal{D}_\mu^\circ$. That means, more vehicles can be served with limited deployment than average demand. So, any demand $\bar{\mathbf{d}} \in \mathcal{D}_\mu^\circ$ can be served without causing the queues to grow to infinity with limited deployment. Therefore, limited deployment satisfies Eq. (19) which makes it a stable control policy for any demand $\bar{\mathbf{d}} \in \mathcal{D}_\mu^\circ$. Following the arguments of remark 2 of Varaiya (2013), from (60) it can further be shown that average queue length of any individual queue in equilibrium is bounded by

$$\frac{1}{M}\mathbb{E}\{\mathbf{x}(t)\} \le \frac{k_1 + k_2^2}{\epsilon} \tag{66}$$

where k_1 and k_2 are constants that depend only on the saturation rates and the maximum demand.

Theorem 3. *There does not exist any signal control under limited budget that can stabilize a network with average demand vector* $\bar{\mathbf{d}} \notin \mathcal{D}_\mu^\circ$

Proof. If $\bar{\mathbf{d}} \notin \mathcal{D}_\mu^\circ$ then we get $\bar{\mathbf{d}} \in \tilde{\mathcal{D}}_\mu$. When $\bar{\mathbf{d}}$ is on the boundary of $\mathcal{D}_\mu^\circ$ the Markov chain representing the queuing model can be null recurrent. For stability the Markov chain is required to be positive recurrent which is implied by Definition 1. So, we consider only the interior $\mathcal{D}'_\mu$ of $\tilde{\mathcal{D}}_\mu$. Then we get

$$\begin{aligned} \mathcal{D}'_\mu = \Big\{ \mathbf{d} : (\bar{\mathbf{f}} = \mathbf{d}\bar{P}) \wedge \Big(& \forall \mathbb{S} \in \mathrm{co}(\mathcal{S}),\ \forall n \in \mathcal{N}^\pi, \exists (i,j) \in \mathcal{M}_n \text{ s.t. } \mathbb{S}_{ij}Q_{ij} < \bar{f}_i \bar{P}_{ij}, \\ & \wedge\ \forall n \in \mathcal{N}^\sigma, \exists (i,j) \in \mathcal{M}_n \text{ s.t. } \bar{S}^\sigma_{ij}Q_{ij} < \bar{f}_i\bar{P}_{ij} \Big)\Big\} \end{aligned} \tag{67}$$

For link $i \in A \setminus \mathcal{A}_\mathrm{r}$ the flow is $f_i(t) = \sum_{h\in\mathcal{I}(i)} y_{hi}(t)$ and Varaiya (2013) showed that the flow for link $i \in \mathcal{A}_\mathrm{r}$ is $f_i(t) = d_i(t)$. Therefore, we can generalize the queueing process given in Eqs. (1) and (2) as the following

$$x_{ij}(t+1) = x_{ij}(t) + f_i(t)P_{ij}(t) - y_{ij}(t) \qquad \forall i \in A\ \forall j \in O(i) \tag{68}$$

Taking the expected value we get

$$\mathbb{E}\left\{x_{ij}(t+1) - x_{ij}(t)\right\} = \mathbb{E}\left\{f_i(t)P_{ij}(t) - y_{ij}(t)\right\} \tag{69}$$

$$\implies \mathbb{E}\left\{x_{ij}(t+1) - x_{ij}(t)\right\} = \mathbb{E}\left\{f_i(t)P_{ij}(t) - \min\left\{x_{ij}(t),\ S^\mu_{ij}(t)Q_{ij}\right\}\right\} \tag{70}$$

Now for any demand vector $\bar{\mathbf{d}} \in \mathcal{D}'_\mu$ there exists a movement (i,j) such that

$$\mathbb{E}\left\{x_{ij}(t+1) - x_{ij}(t)\right\} > \bar{f}_i\bar{P}_{ij} - \bar{S}^\mu_{ij}Q_{ij} > 0 \tag{71}$$

However, Eq. (71) implies increasing queue length at every timestep on average for at least one movement (i,j) which violates Definition 1. Therefore if $\bar{d} \notin \mathcal{D}_\mu^\circ$ the network cannot be stabilized by any control. □

Corollary 1. *Limited deployment control is maximally stable.*

Proof. Theorem 2 showed that if $\bar{\mathbf{d}} \in \mathcal{D}^{\circ}_{\mu}$ then the limited deployment can stabilize the network. Theorem 3 showed that if $\bar{\mathbf{d}} \notin \mathcal{D}^{\circ}_{\mu}$ then no control can stabilize the network. Therefore, limited deployment control can stabilize all possibly stabilizable demands. □

4. Limited deployment formulation

Having shown that under limited deployment $\mathcal{N} = \mathcal{N}^{\sigma} \cup \mathcal{N}^{\pi}$, max-pressure control will stabilize any demand $\bar{\mathbf{d}}$ in the restricted stability region $\mathcal{D}^{\circ}_{\mu}$ the natural objective is to select $\mathcal{N}^{\pi} \subseteq \mathcal{N}$ to optimize $\mathcal{D}^{\circ}_{\mu}$. While $\mathcal{N}^{\pi} = \mathcal{N}$ is ideal, budget limitations may render it impractical. Furthermore, demand for some intersections may be sufficiently small that replacing their signal control hardware has little practical benefit. We formulate a mixed integer linear program to identify the highest-priority intersections to implement max-pressure control.

4.1. Demand maximization under limited budget

Let $\gamma_n \in \{0,1\}$ indicate whether the intersection control at node n is updated and let b_n be the cost of updating node n with a total budget limitation of B. If n is updated, then the default control at n of $\tilde{S}_n$ can be replaced with some $\bar{S}_n \in \mathrm{co}(\mathcal{S}_n)$. This choice can be represented by the following constraints.

$$\bar{f}_i = \bar{d}_i \qquad \forall i \in \mathcal{A}_{\mathrm{r}} \tag{72a}$$

$$\bar{f}_j = \sum_{i \in I(n)} \bar{f}_i \bar{P}_{ij} \qquad \forall j \in \mathcal{A}_{\mathrm{i}} \cup \mathcal{A}_{\mathrm{s}} \tag{72b}$$

$$f_i P_{ij} \le Q_{ij} \bar{S}_{ij} \qquad \forall n \in \mathcal{N},\ \forall i \in I(n),\ \forall j \in \mathcal{O}(i) \tag{72c}$$

$$\bar{S}_{ij} = \sum_{S \in \mathcal{S}_n} \lambda_S S_{ij} \qquad \forall n \in \mathcal{N},\ \forall i \in I(n),\ \forall j \in \mathcal{O}(i) \tag{72d}$$

$$\sum_{S \in \mathcal{S}_n} \lambda_S \le 1 \qquad \forall n \in \mathcal{N} \tag{72e}$$

$$\gamma_n \ge \bar{S}_{ij} - \tilde{S}_{ij} \qquad \forall n \in \mathcal{N},\ \forall i \in I(n),\ \forall j \in \mathcal{O}(i) \tag{72f}$$

$$\gamma_n \ge \tilde{S}_{ij} - \bar{S}_{ij} \qquad \forall n \in \mathcal{N},\ \forall i \in I(n),\ \forall j \in \mathcal{O}(i) \tag{72g}$$

$$\gamma_n \in \{0,1\} \qquad \forall n \in \mathcal{N} \tag{72h}$$

Constraint (72c) is the stable region constraint used in Eq. (18), and constraints (72d) and (72e) relate $\bar{S}_{ij}$ to the definition of the convex hull. Constraints (72f) and (72g) force $\gamma_n = 1$ if $\bar{S}_{ij} \neq \tilde{S}_{ij}$ (i.e. the signal timing is changed due to implementing max-pressure control). The budget constraint can be written as

$$\sum_{n \in \mathcal{N}} b_n \gamma_n \le B \tag{73}$$

If the objective is to maximize the demand that can be served, then the problem can be solved by the following mixed-integer-linear-program (MILP):

$$\max \sum_{i \in \mathcal{A}_{\mathrm{r}} \cup \mathcal{A}_{\mathrm{s}}} d_i \tag{74}$$

$$\text{s.t.} \quad (72a)–(72b),\ (72c)–(72h),\ (73)$$

Problem (74) is a simple approach to optimizing the number of vehicles that can be served. However, demand is typically origin–destination based in nature, so maximizing the total demand that is served may not be useful if travelers are not interested in those origin–destination proportions of travel.

4.2. Demand maximization according to origin–destination proportions under limited budget

Suppose that vehicular demand enters at the ratios of $\hat{\mathbf{d}}$. A natural objective is to serve as large a proportion of this demand as possible, i.e. max α where actual demand is $\alpha\hat{\mathbf{d}}$. Using Eqs. (72a) and (72b), this demand can be distributed over links as

$$\alpha \hat{f}_i = \alpha \hat{d}_i \qquad \forall i \in \mathcal{A}_{\mathrm{r}} \cup \mathcal{A}_{\mathrm{s}} \tag{75a}$$

$$\alpha \hat{f}_j = \alpha \sum_{i \in \mathcal{I}(j)} \hat{f}_i P_{ij} \qquad \forall j \in \mathcal{A}_{\mathrm{i}} \tag{75b}$$

with the amount of demand that can be served by limited deployment of max-pressure controls

$$\alpha \hat{f}_i P_{ij} \le Q_{ij} \bar{S}_{ij} \qquad \forall n \in \mathcal{N}, \forall (i,j) \in \mathcal{M}_n \tag{76}$$

This results in the following MILP:

$$\max \quad \alpha \tag{77a}$$

$$\text{s.t.} \quad \alpha \leq \alpha_n \qquad \forall n \in \mathcal{N} \tag{77b}$$

$$\hat{f}_i = \hat{d}_i \qquad \forall i \in \mathcal{A}_{\mathrm{r}} \cup \mathcal{A}_{\mathrm{s}} \tag{77c}$$

$$\hat{f}_j = \sum_{i \in \mathcal{I}(j)} \hat{f}_i P_{ij} \qquad \forall j \in \mathcal{A}_{\mathrm{i}} \tag{77d}$$

(72d)–(72h), (73), (76)

(77b) ensures that the system-wide α is bounded by the lowest α_n. So, the maximization problem improves the lowest α_n by installing MP control thus increasing system-wide α. This constraint enables a greedy algorithm to solve this problem because we can just find the next lowest α_n and if MP control is not installed there we can improve the system-wide α. Since constraints (77c) and (77d) are independent of α, they can be solved separately. Then, constraint (76) can be solved to find the maximum α_n possible for each n. Because the overall system-wide α is limited by the smallest α_n, we present a decentralized greedy algorithm to solve the problem (77a). Algorithm 1 works by setting the signal capacity at each node initially equal to its current available capacity. Then, Algorithm 1 improves the node n' with active constraint (77b) until the maximum budget B is exhausted. Due to constraint (77b), improving any other node (although it may be more budget-efficient) would not yield an improvement on the overall α. Since MILP's are NP-hard, having a polynomial-time algorithm that can solve the problem to optimality ensures better computation time. Solving this problem with an algorithm like branch and bound may require exploring all possible permutation of MP control installation in the worst case, where the cardinality of permutation is equal to B. The time complexity of such algorithms are typically exponential. However, the greedy algorithm only requires solving B LP's ($B \in \mathbb{Z}_+$ and each MP control installation incurs 1 unit cost). According to Cohen et al. (2018), LP's can be solved in current matrix multiplication time $O(n^{\omega})$ where $\omega \approx 2.373$. Therefore, the computational complexity of the greedy method is $O(Bn^{\omega})$ which is better than exponential time.

Algorithm 1 Greedy algorithm to optimize max-pressure installations to find maximum α ratio of served demand.

1: Solve eq. (77c) and eq. (77d) to obtain $\hat{f}_i \; \forall i \in A_{all}$
2: **for** $n \in N$ **do**
3: $\quad \bar{S}_n \leftarrow \tilde{S}_n$
4: **end for**
5: **while** $B > 0$ **do**
6: $\quad n' \leftarrow \underset{n \in N}{\operatorname{argmin}} \left\{ \max \left\{ \alpha_n : \alpha_n \hat{f}_i P_{ij} < Q_{ij} \bar{S}_n(i,j) \quad \forall (i,j) \in \mathcal{M}_n \right\} \right\}$
7: $\quad$ **if** $b_{n'} \leq B$ **then**
8: $\qquad \bar{S}_{n'} \leftarrow \underset{\hat{S}_{n'} \in \mathrm{co}(\hat{S}_{n'})}{\operatorname{argmax}} \left\{ \alpha_n : \alpha_n \hat{f}_i P_{ij} < Q_{ij} \hat{S}_{n'}(i,j) \quad \forall (i,j) \in \mathcal{M}_{n'} \right\}$
9: $\qquad B \leftarrow B - b_{n'}$
10: $\quad$ **else**
11: $\qquad$ break
12: $\quad$ **end if**
13: **end while**

Theorem 4. *If for a given budget, B the solution from Algorithm 1 is γ' and a global optimal solution is γ^* then $\gamma' = \gamma^*$.*

Proof. By contradiction. Let γ' be the solution from Algorithm 1 and let γ^* be a globally optimal solution with $\alpha^* > \alpha'$.

Case 1: Suppose that $\gamma'_n = 1$ but $\gamma^*_n = 0$. Then $\alpha^* \leq \alpha_n$ by constraint (1), but $\alpha_n \leq \alpha'$ because Algorithm 1 selects nodes that lower bound α' in line 6 of Algorithm 1. Then, $\alpha^* \leq \alpha_n \leq \alpha'$, which contradicts $\alpha^* > \alpha'$.

Case 2: Suppose that $\gamma'_n = 0$ but $\gamma^*_n = 1$. The Algorithm 1 terminates if budget is exhausted or less than the smallest MP installation cost according to line 5 and line 7 of Algorithm 1. So, at termination of Algorithm 1, either all nodes use max pressure control or there is insufficient budget to improve α. Therefore, $\gamma' = \gamma^*$. □

5. Numerical results

To demonstrate the results, we use the downtown Austin city network which was calibrated to match observed morning peak characteristics in 2011 by the Network Modeling Center at the University of Texas at Austin (Levin et al., 2020). This network consists of 171 zones, 546 intersections, 150 signalized intersections and 1247 links. This network also includes most of the central business district of Austin, Texas. Arterials north of the city and the two major north-south freeways are also included in this network. The network data also includes signal timings for the signalized intersections. All of the simulations used a MP timestep of 15 seconds and a total duration of 3 hours. All links were modeled using a point queue link model in simulation. Fig. 1 shows the downtown Austin network with the MP control and signal control obtained from Austin network dataset shown by the red and green nodes respectively.

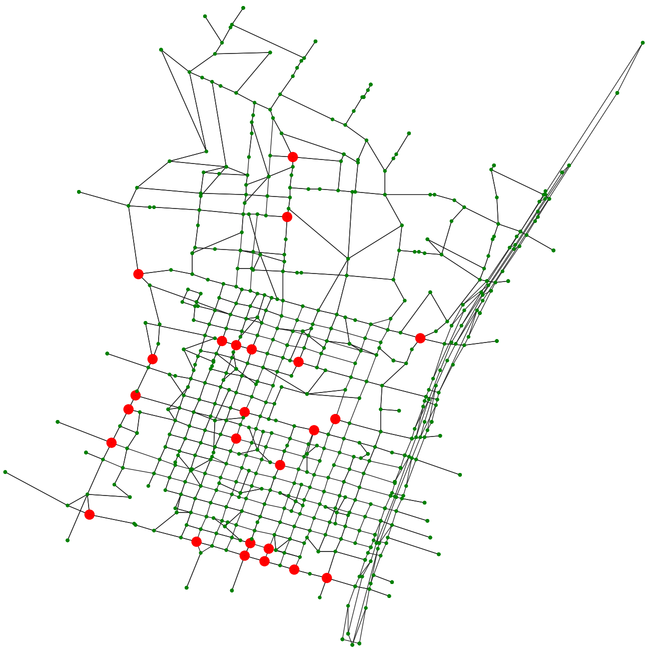

Fig. 1. Downtown Austin network, red nodes are MP controlled and other nodes are controlled using timings from Austin network data.

To obtain the turning proportions, we solved dynamic traffic assignment (DTA) using the method of successive averages. The DTA was run in a custom in-house simulator called AVDTA written in Java. The point queue link model was used in our simulator. As part of our analysis of maximum stable demand from simulations, we needed to develop an automated stability detection procedure which will be discussed in detail, later in this section. This new stability detection procedure can however be very sensitive. In the absence of a more robust stability detection methodology in the literature, we wanted to minimize the difference between the traffic flow models used in the proofs and the simulations. Because, using the point queue model in simulations instead of a more realistic model would help ensure any difference between theoretical (from MILP) and simulation results for the maximum stable demand was caused by the sensitivity in stability detection. Therefore, to ensure that the assumption about traffic conditions in the simulations matched our assumptions for the theoretical model, we wrote code to modify our custom simulator AVDTA in Java. We implemented the point queue link model as it is described in theory. The sending and receiving flow calculation in our simulator are exactly the same as that of the point queue link model. Again, this was done to ensure consistency of assumption about traffic and minimum difference between the theoretical and simulation results. Under different realizations of demands, the simulation and the theoretical maximum stable demand were observed to be similar. The only source of difference here was the sensitivity of stability detection. The optimization problem Eq. (77a) is then solved using Algorithm 1 and these turning proportions to find the intersections where MP control should be installed. These MP control intersections are shown in Fig. 1 by red nodes.

To verify the accuracy of this result and to show the benefits of installing max pressure control on more nodes we ran simulations using AVDTA. We created simulations in AVDTA and determined the maximum stable demands using subsets of limited deployment nodes. From this point on the sum of the demands for the entry links will be referred to as the demand. So, the maximum stable demand would be the sum of the demands for all the entry links that can be stabilized. We also deployed MP in random nodes and determined the maximum stable demands for those MP installations. We then compared the maximum stable demands with limited deployment and random deployment of MP control. We used the point queue link model in AVDTA because we used that model in our proof of stability. In the simulations, MP control is implemented in the intersections found by solving the MILP using Algorithm 1. To control all the other intersections, the pretimed signal timings data already available for the Austin network were used. Each intersection was controlled separately in simulation. For each non-MP controlled intersection, at every simulation step it was checked whether the allocated time for the active phase ran out or not. If the time for the active phase ran out then the next phase was activated. Similarly, for the MP controlled intersections, at every simulation step it was checked whether the MP timestep of 15 seconds ran out. If that MP timestep became zero at a simulation step, then for that intersection the MP control algorithm was called to find and activate the next optimal phase.

First, 20 intersections selected by the optimization problem were chosen where MP control was implemented and in the other signalized intersections the original signal timings provided in the Austin network data were used. Denote this set of 20 nodes selected by the limited deployment nodes set by N_{ld}. We also denote the sum of maximum stable demand by $h_{|n|}$ for nodes $n \subset N_{\text{ld}}$. To find the $h_{|n|}$ we formulate a decision problem: given some sum of demands for the entry links d and the AVDTA simulator as the verifier, can d be stabilized or is $d \leq h_{|n|}$? We assume that any sum of demands $d \leq h_{|n|}$ can be stabilized and $d > d^{s}_{|n|}$ cannot be stabilized. Using this assumption and the decision problem, we perform binary search for the maximum stable demands sum for

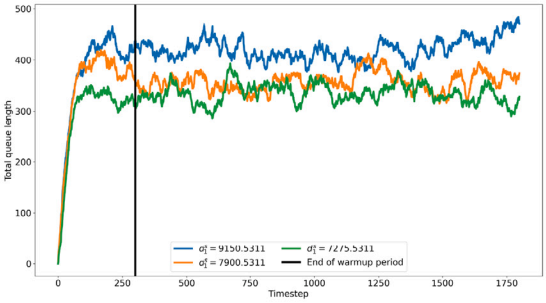

(a) Deployment of 1 MP control

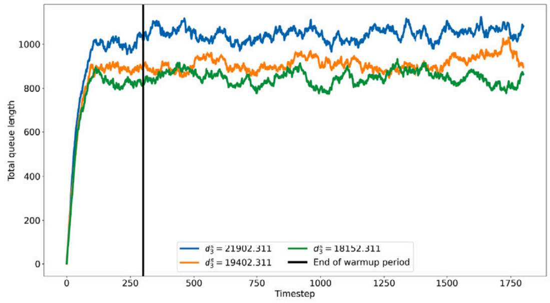

(b) Deployment of 3 MP controls

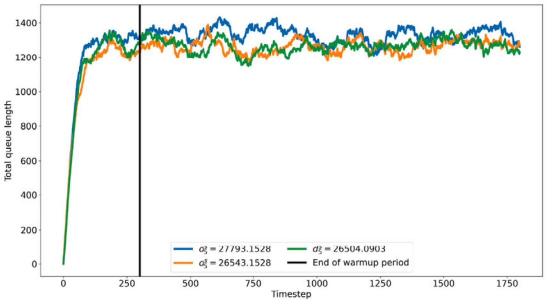

(c) Deployment of 5 MP controls

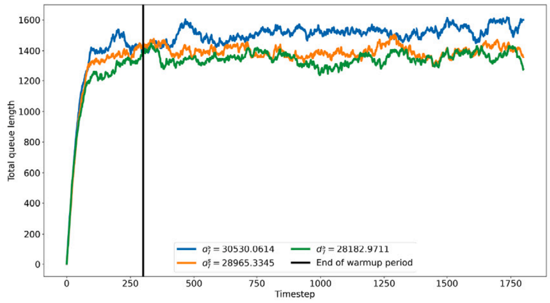

(d) Deployment of 7 MP controls

Fig. 2. Stability detection by binary search for different deployments of MP control (Data from only 1 repetition of MC is plotted.).

$n \subset N_{\text{ld}}$. For a limited deployment of $n \subset N_{\text{ld}}$ nodes where MP is installed, we define the stable demand sum $h_{|n|}$ from the verifier AVDTA simulator as: $h_{|n|}$ is stable if the best fitted line of the sum of queue lengths at time t, over the period starting from after a warmup period w to the end of simulation has a slope less than some maximum predefined slope $s \in \mathbb{R}_+$. This definition ensures that the queue length will not grow to infinity with progression in time which is consistent with the formal definition of stability given in Definition 1. Similarly, we also find the maximum stable demands for random deployment of MP control.

We ran Monte Carlo (MC) simulations with 100 repetitions to decrease the effects of stochasticity while trying to find the stable demands. During our first run of the simulations, we noticed that after about 200 timesteps the fluctuations in the queue length were not that large compared to before that warmup period. This is because during the first 200 timesteps the there was plenty of space in the network for the vehicles to enter. After the 200 timesteps however, some vehicles needed to exit to make space for new vehicles to enter the network. To be safe we selected this warmup period to be 300 timesteps for all the simulations. The large change in queue length before the 200 timesteps can be seen in Fig. 2. Fig. 2 further shows how queue lengths fluctuates for different total demands under different deployments. Analyzing these fluctuations help us detect stability and whether a d_n^s is in the set of feasible demands. The curves corresponding to different d_n^s that do not have a high increasing trend indicate that for those different total demands the network can be stabilized. To detect the feasible demands binary search with different total demands were done for different deployments. Some of the queue length fluctuations from those simulation runs are presented in Fig. 2, mainly to provide visualization to help describe how stability detection works. For the maximum slope s of the fitted line (for different curves some of which are presented in Fig. 2) we tested several values. Using those values, we determined stability for different deployments and plotted the maximum stable demands in Fig. 3. The maximum slope needed to be very small to ensure that the fitted straight line is close to horizontal which would indicate stability. However, a slight positive slope is allowable since over a period of 3 hours if the total average queue length increases by $1-5$ vehicles then the demand can still be reasonably considered to be stable. We used two slopes, 0.0001 and 0.0005 which approximately translates to an increase of 1 and 5 vehicles over the 3 h simulation period respectively. Manual human inspection of the stability plots can be done to detect stability with higher accuracy. However, we had to run many simulations to find the maximum stable demands and manually inspecting each of those simulation was not feasible. In addition, to ensure reproducibility of results we avoided manual human inspection to determine stability and used the maximum slopes. Further research should address this issue of stability detection. For a split of 0.50 if at least 50% repetitions of a simulation for a demand were stable then that demand was considered to be stabilizable otherwise unstabilizable. We used this split of 0.5 to also reduce the number of simulations that needed to be run. For example, if more than 50% of the times realizations of demands led to a stable network then we could say majority of the times the realizations of the average demand were observed to be stable. Running further simulations will not change the majority results, so further simulations does not need to be run. Since detection of stability is very sensitive, we also used a split of 0.40. Therefore, if a demand was identified to be stable for 40% of the MC repetitions then that demand would be considered stable.

The theoretical stable demand sum for limited deployment of n nodes line in Fig. 3 shows that after installing MP in 7 nodes, more MP installations did not result in significant increase in maximum stable demand. This is because the system wide α is lower

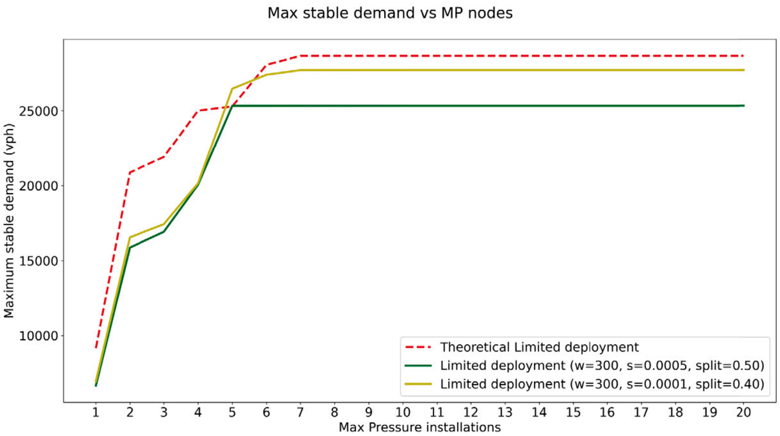

Fig. 3. Maximum stable demands achieved with different deployment policies of MP nodes.

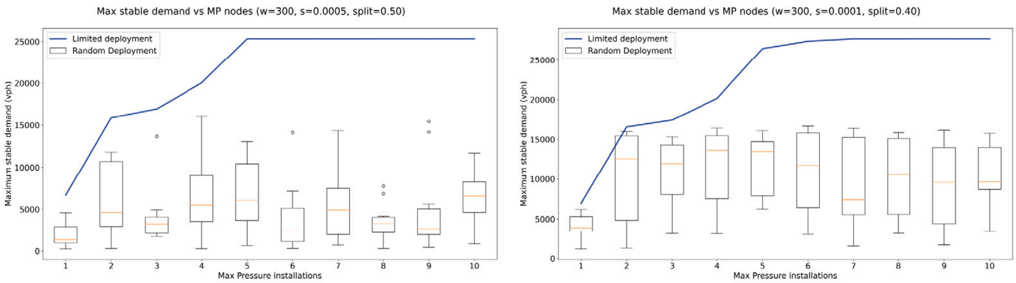

Fig. 4. Maximum stable demands achieved with different deployment policies of MP nodes.

bounded by the minimum α_n. Therefore, even if installation of MP control results in increase of α_n in node n it will not increase the system wide α if another node n' where MP is already installed has $\alpha_{n'} = \alpha$ and $\alpha_{n'} < \alpha_n$. This means even though installing MP in a node may increase its performance in terms of throughput, the maximum stable demand may still be bounded. This number of 7 intersections however is dependent on the geometry of the network and historical turn proportions. Since the greedy algorithm will choose the next optimal location to maximize proportion of demand served the sequence of optimal locations to install MP control will remain the same for the same network geometry with the same historical turn proportions. With different choice of parameters, the stability detection method caused the binary search to converge to different maximum stable demands as shown in Fig. 3. The pattern in which the maximum stable demand changed however was mostly similar to theoretical results. With a warmup, maximum slope and split of 300 timesteps, 0.0005, 0.50 respectively, the trend of increase in maximum stable demand followed theoretical results except for the change from 4 to 5 deployed nodes. Fig. 3 shows that theoretical limited deployment predicted a much flatter increase where simulation determined a much steeper increase in the maximum stable demand. The optimization problem considers average signal timing for MP control and but the simulation was only repeated a limited number of times and also the stability detection method not being perfect may explain this discrepancy.

Then we selected random nodes to install MP control and then determined the maximum stable demand using the same method. Fig. 4 shows the maximum stable demands for both limited and random deployment of MP controlled nodes. For the random deployment, the same stability detection parameters were used. Fig. 4 shows that with the same stability detection parameters limited deployment was able to stabilize more demand than random deployment. So, even though stability detection is not perfect using the same parameters for stability detection, limited deployment performed better than random deployment to increase system performance.

The maximum stable demand bound does not mean installing max pressure control in more nodes will not result in more benefits. We used Monte Carlo simulations with 10 repetitions to demonstrate the impacts of limited deployment of up to 100 nodes on different aspects of network performance. We ran these simulations with a fixed number of vehicles inserted per hour into the network. The other parameters of the simulations were kept unchanged.

Fig. 5 shows decreasing trends in total average queue length, average travel times and link densities as deployment of MP control increases. For higher demand even installing MP control in a few intersections yielded better performance which is consistent with our theory. Fig. 3 shows that deployment of MP control resulted in high increase in maximum stable demand in the beginning but after a certain number of installations the maximum stable demand could not be increased anymore. Fig. 5 shows a similar pattern.

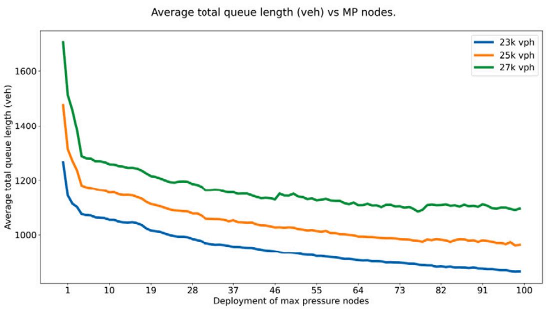

(a) Average total queue length with increase in limited deployment.

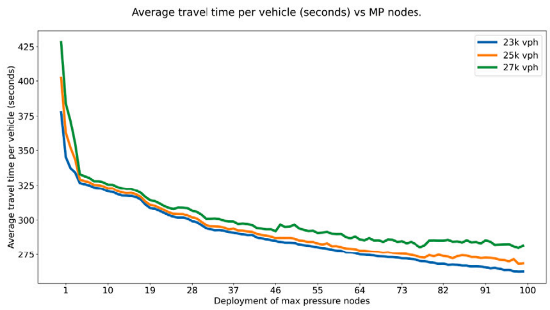

(b) Average travel time per vehicle with increase in limited deployment.

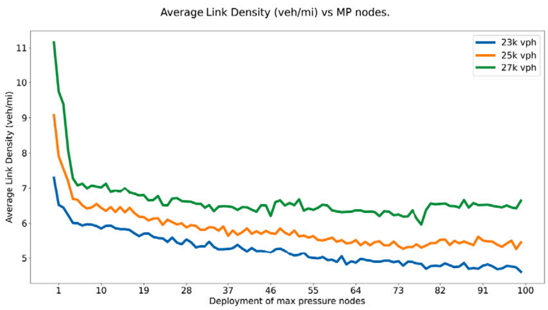

(c) Average link density with increase in limited deployment.

Fig. 5. Change in different performance metrics with increase in limited deployment.

Since the maximum stable demand becomes bounded after a certain number of MP control installations the performance benefits resulting from more MP control deployment do not increase as much anymore. However, a small increase in benefits with more MP controllers is still noticeable from Fig. 5. In particular, the decrease in average travel time per vehicle demonstrates how limited deployment of MP controls benefit the system performance. These results indicate that as the deployment of MP control increases the system performance also increases. System performance depends on the maximum stabilizable demands which is also shown to increase with limited deployment.

6. Conclusions

This paper discussed the problem of deployment of MP controls under limited budget. Previous studies proved that the MP control is throughput maximizing with the condition that all of the signalized intersections use MP control. However, installing MP control in all intersections may not be possible considering budget limitations. Therefore, this paper analyzed whether MP control can still guarantee maximum throughout with limited deployment. We showed that even with limited deployment MP control can still achieve maximum throughput, but with less MP controlled intersections the stable region is smaller. Then we presented a MILP to find the optimal intersections to install MP control. We designed a greedy algorithm to solve the MILP efficiently and proved that it can solve the problem to optimality. Using that problem, we determined the theoretical maximum stable demands for deployment of MP controllers under different budgets. We presented how maximum stable demand from simulations can be determined using a search algorithm using a decision problem and the simulator. Then we ran simulations with Monte Carlo repetitions in AVDTA, our custom simulator to verify the theoretical results. After analyzing the downtown Austin network, we found that after installing MP control in only a few intersections most of the maximum stabilizable demand from standard MP control could be served. We then compared and showed how the theoretical results mostly matched with the results from the simulator. We also ran simulations with fixed demands and increasing number of MP control deployments to see its effect on system performance. The decrease in average queue length and link density shows the network benefits and the decrease in average travel time per vehicle shows how limited deployment benefits the travelers. We found that installing more MP controls after reaching the maximum stabilizable demand further increased the system performance. Therefore, installing more MP controls is desirable.

In this paper, we assumed the point queue link model which does not describe the traffic conditions perfectly. Future work should focus on analyzing the stability properties and conducting simulations with a more realistic link model. More networks with different network geometries should be analyzed numerically. Combinations of deployment of MP control and multiple other controllers should also be studied to see if system performance can be improved. Considering pedestrian traffic and explicit signal coordination between intersections with same or different types of controllers should be interesting to study. How different levels of market penetration of CAV's would affect limited deployment of MP control should also be an interesting and realistic problem to consider. Since MP control relies heavily on sensors to detect queue lengths it can be vulnerable to cyber-attacks. Methods of detecting such attacks and designing fail-safe controls should also be studied.

CRediT authorship contribution statement

Simanta Barman: Conceptualization, Methodology, Software, Formal analysis, Investigation, Writing – original draft, Writing – review & editing, Visualization. **Michael W. Levin:** Supervision, Conceptualization, Methodology, Software, Writing – review & editing.

References

Anderson, Leah, Pumir, Thomas, Triantafyllos, Dimitrios, Bayen, Alexandre M., 2018. Stability and implementation of a cycle-based max pressure controller for signalized traffic networks. Netw. Heterog. Media 13 (2), 241.

Barman, Simanta, Levin, Michael W., 2022. Performance evaluation of modified cyclic max-pressure controlled intersections in realistic corridors. Transp. Res. Rec. 2676 (6), 110–128. http://dx.doi.org/10.1177/03611981211072807.

Cao, Jingnan, Hu, Yonghui, Diamantis, Manolis, Zhang, Siyu, Wang, Yibing, Guo, Jingqiu, Papamichail, Ioannis, Papageorgiou, Markos, Zhang, Lihui, Hu, Jun Simon, 2020. A max pressure approach to urban network signal control with queue estimation using connected vehicle data. In: 2020 IEEE 23rd International Conference on Intelligent Transportation Systems. ITSC, IEEE, pp. 1–8.

Chang, Wanli, Roy, Debayan, Zhao, Shuai, Annaswamy, Anuradha, Chakraborty, Samarjit, 2020. Cps-oriented modeling and control of traffic signals using adaptive back pressure. In: 2020 Design, Automation & Test in Europe Conference & Exhibition. DATE, IEEE, pp. 1686–1691.

Chen, Rongsheng, Hu, Jeffrey, Levin, Michael W., Rey, David, 2020. Stability-based analysis of autonomous intersection management with pedestrians. Transp. Res. C 114, 463–483.

Chong, Edwin K.P., Zak, Stanislaw H., 2004. An Introduction to Optimization. John Wiley & Sons.

Cohen, Michael B., Lee, Yin Tat, Song, Zhao, 2018. Solving linear programs in the current matrix multiplication time. CoRR, abs/1810.07896. URL http://arxiv.org/abs/1810.07896.

Dixit, Vinayak, Nair, Divya Jayakumar, Chand, Sai, Levin, Michael W., 2020. A simple crowdsourced delay-based traffic signal control. PLoS One 15 (4), e0230598.

Gregoire, Jean, Frazzoli, Emilio, de La Fortelle, Arnaud, Wongpiromsarn, Tichakorn, 2014a. Back-pressure traffic signal control with unknown routing rates. CoRR, abs/1401.3357. URL http://arxiv.org/abs/1401.3357.

Gregoire, Jean, Qian, Xiangjun, Frazzoli, Emilio, De La Fortelle, Arnaud, Wongpiromsarn, Tichakorn, 2014b. Capacity-aware backpressure traffic signal control. IEEE Trans. Control Netw. Syst. 2 (2), 164–173.

Gregoire, Jean, Samaranayake, Samitha, Frazzoli, Emilio, 2016. Back-pressure traffic signal control with partial routing control. In: 2016 IEEE 55th Conference on Decision and Control. CDC, IEEE, pp. 6753–6758.

Hao, ShenXue, Yang, LiCai, 2019. Traffic network modeling and extended max-pressure traffic control strategy based on granular computing theory. Math. Probl. Eng. 2019.

Hoffman, A.J., Kruskal, J.B., 2016. 13. Integral Boundary Points of Convex Polyhedra. Princeton University Press, pp. 223–246. http://dx.doi.org/10.1515/9781400881987-014.

Kang, Di, Levin, Michael W., 2021. Maximum-stability dispatch policy for shared autonomous vehicles. Transp. Res. B 148, 132–151.

Kouvelas, Anastasios, Lioris, Jennie, Alireza Fayazi, S., Varaiya, Pravin, 2014. Maximum pressure controller for stabilizing queues in signalized arterial networks. Transp. Res. Rec. 2421 (1), 133–141. http://dx.doi.org/10.3141/2421-15.

Le, Tung, Kovács, Péter, Walton, Neil, Vu, Hai L., Andrew, Lachlan L.H., Hoogendoorn, Serge S.P., 2015. Decentralized signal control for urban road networks. Transp. Res. C 58, 431–450.

Levin, Michael W., Boyles, S., 2017. Pressure-based policies for reservation-based intersection control. In: 96th Annual Meeting of the Transportation Research Board. Washington, DC.

Levin, Michael W., Hu, Jeffrey, Odell, Michael, 2020. Max-pressure signal control with cyclical phase structure. Transp. Res. C (ISSN: 0968-090X) 120, 102828. http://dx.doi.org/10.1016/j.trc.2020.102828, URL https://www.sciencedirect.com/science/article/pii/S0968090X20307324.

Levin, Michael W., Rey, David, Schwartz, Adam, 2019. Max-pressure control of dynamic lane reversal and autonomous intersection management. Transp. B Transp. Dyn. 7 (1), 1693–1718.

Li, Li, Jabari, Saif Eddin, 2019. Position weighted backpressure intersection control for urban networks. Transp. Res. B 128, 435–461.

Li, Li, Pantelidis, Theodoros, Chow, Joseph Y.J., Jabari, Saif Eddin, 2021. A real-time dispatching strategy for shared automated electric vehicles with performance guarantees. Transp. Res. E 152, 102392.

Lioris, Jennie, Kurzhanskiy, Alex, Varaiya, Pravin, 2016. Adaptive max pressure control of network of signalized intersections. IFAC-PapersOnLine (ISSN: 2405-8963) 49 (22), 19–24. http://dx.doi.org/10.1016/j.ifacol.2016.10.366, https://www.sciencedirect.com/science/article/pii/S240589631631953X.

Liu, Ying, Gao, Juntao, Ito, Minoru, 2018. Back-pressure based adaptive traffic signal control and vehicle routing with real-time control information update. In: 2018 IEEE International Conference on Vehicular Electronics and Safety. ICVES, IEEE, pp. 1–6.

Mercader, Pedro, Uwayid, Wasim, Haddad, Jack, 2020. Max-pressure traffic controller based on travel times: An experimental analysis. Transp. Res. C 110, 275–290.

Nilsson, Gustav, Como, Giacomo, 2020. A micro-simulation study of the generalized proportional allocation traffic signal control. IEEE Trans. Intell. Transp. Syst. (ISSN: 1558-0016) 21 (4), 1705–1715. http://dx.doi.org/10.1109/TITS.2019.2957718.

Nilsson, Gustav, Como, Giacomo, 2022. Generalized proportional allocation policies for robust control of dynamical flow networks. IEEE Trans. Automat. Control (ISSN: 1558-2523) 67 (1), 32–47. http://dx.doi.org/10.1109/TAC.2020.3046026.

Pumir, Thomas, Anderson, Leah, Triantafyllos, Dimitrios, Bayen, Alexandre M., 2015. Stability of modified max pressure controller with application to signalized traffic networks. In: 2015 American Control Conference. ACC, IEEE, pp. 1879–1886.

Ramadhan, S.A., Sutarto, H.Y., Kuswana, G.S., Joelianto, E., 2020. Application of area traffic control using the max-pressure algorithm. Transp. Plan. Technol. 43 (8), 783–802.

Rey, David, Levin, Michael W., 2019. Blue phase: Optimal network traffic control for legacy and autonomous vehicles. Transp. Res. B 130, 105–129.

Robbennolt, Jake, Chen, Rongsheng, Levin, Michael, 2022. Microsimulation study evaluating the benefits of cyclic and non-cyclic max-pressure control of signalized intersections. Transp. Res. Rec. 03611981221095520.

Sha, Rui, Chow, Andy H.F., 2019. A comparative study of centralised and decentralised architectures for network traffic control. Transp. Plan. Technol. 42 (5), 459–469.

Smith, Michael J., Iryo, Takamasa, Mounce, Richard, Rinaldi, Marco, Viti, Francesco, 2019. Traffic control which maximises network throughput: Some simple examples. Transp. Res. C 107, 211–228.

Sun, Xiaotong, Yin, Yafeng, 2018. A simulation study on max pressure control of signalized intersections. Transp. Res. Rec. 2672 (18), 117–127.

Taale, Henk, van Kampen, Joost, Hoogendoorn, Serge, 2015. Integrated signal control and route guidance based on back-pressure principles. Transp. Res. Procedia 10, 226–235.

Tassiulas, L., Ephremides, A., 1992. Stability properties of constrained queueing systems and scheduling policies for maximum throughput in multihop radio networks. IEEE Trans. Automat. Control 37 (12), 1936–1948. http://dx.doi.org/10.1109/9.182479.

Varaiya, Pravin, 2013. Max pressure control of a network of signalized intersections. Transp. Res. C 36, 177–195.

Vickrey, William S., 1963. Pricing in urban and suburban transport. Am. Econ. Rev. (ISSN: 00028282) 53 (2), 452–465, URL http://www.jstor.org/stable/1823886.

Wongpiromsarn, Tichakorn, Uthaicharoenpong, Tawit, Wang, Yu, Frazzoli, Emilio, Wang, Danwei, 2012. Distributed traffic signal control for maximum network throughput. In: 2012 15th International IEEE Conference on Intelligent Transportation Systems. pp. 588–595. http://dx.doi.org/10.1109/ITSC.2012.6338817.

Wu, Jian, Ghosal, Dipak, Zhang, Michael, Chuah, Chen-Nee, 2018. Delay-based traffic signal control for throughput optimality and fairness at an isolated intersection. IEEE Trans. Veh. Technol. 67 (2), 896–909. http://dx.doi.org/10.1109/TVT.2017.2760820.

Xiao, Nan, Frazzoli, Emilio, Li, Yitong, Luo, Yiwen, Wang, Yu, Wang, Danwei, 2015a. Further study on extended back-pressure traffic signal control algorithm. In: 2015 54th IEEE Conference on Decision and Control. CDC, pp. 2169–2174. http://dx.doi.org/10.1109/CDC.2015.7402528.

Xiao, Nan, Frazzoli, Emilio, Li, Yitong, Wang, Yu, Wang, Danwei, 2014. Pressure releasing policy in traffic signal control with finite queue capacities. In: 53rd IEEE Conference on Decision and Control. IEEE, pp. 6492–6497.

Xiao, Nan, Frazzoli, Emilio, Luo, Yiwen, Li, Yitong, Wang, Yu, Wang, Danwei, 2015b. Throughput optimality of extended back-pressure traffic signal control algorithm. In: 2015 23rd Mediterranean Conference on Control and Automation. MED, pp. 1059–1064. http://dx.doi.org/10.1109/MED.2015.7158897.

Xiao, Jiawang, Song, Xiang Ben, Ma, Xiaolong, Jin, Sheng, 2020. A back-pressure-based model with fixed phase sequences for traffic signal optimization under oversaturated networks. IEEE Trans. Intell. Transp. Syst. 1–12. http://dx.doi.org/10.1109/TITS.2020.2987917.

Xu, Te, Barman, Simanta, Levin, Michael W., Chen, Rongsheng, Li, Tianyi, 2022. Integrating public transit signal priority into max-pressure signal control: Methodology and simulation study on a downtown network. Transp. Res. C 138, 103614.

Xu, Te, Levin, Michael W., Cieniawski, Maria, 2021a. A zone-based dynamic queueing model and maximum-stability dispatch policy for shared autonomous vehicles. In: 2021 IEEE International Intelligent Transportation Systems Conference. ITSC, pp. 3827–3832. http://dx.doi.org/10.1109/ITSC48978.2021.9565127.

Xu, Yunwen, Li, Dewei, Xi, Yugeng, Lin, Shu, 2021b. Path-based adaptive traffic signal control with a mixed backpressure index. In: 2021 IEEE International Intelligent Transportation Systems Conference. ITSC, IEEE, pp. 2484–2491.

Yen, Chia-Cheng, Ghosal, Dipak, Zhang, Michael, Chuah, Chen-Nee, Chen, Hao, 2018. Falsified data attack on backpressure-based traffic signal control algorithms. In: 2018 IEEE Vehicular Networking Conference. VNC, pp. 1–8. http://dx.doi.org/10.1109/VNC.2018.8628334.

Yu, Hao, Liu, Pan, Fan, Yueyue, Zhang, Guohui, 2021. Developing a decentralized signal control strategy considering link storage capacity. Transp. Res. C 124, 102971.

Zhang, Siyu, Diamantis, Manolis, Wang, Yibing, Guo, Jingqiu, Papamichail, Ioannis, Papageorgiou, Markos, Zhang, Lihui, Hu, Jun Simon, 2020. Joint queue estimation and max pressure control for signalized urban networks with connected vehicles. In: 2020 Forum on Integrated and Sustainable Transportation Systems. FISTS, IEEE, pp. 211–217.